MCB
Journals.ASM.org

Regulation of Ras Localization and Cell Transformation by Evolutionarily Conserved Palmitoyltransferases

Evelin Young,[a,b] Ze-Yi Zheng,[a,b] Angela D. Wilkins,[c,d] Hee-Tae Jeong,[a,b] Min Li,[e] Olivier Lichtarge,[c,d] Eric C. Chang[a,b]

Department of Molecular and Cellular Biology,[a] Lester and Sue Smith Breast Center,[b] Department of Molecular and Human Genetics,[c] and CIBR Center for Computational and Integrative Biomedical Research,[d] Baylor College of Medicine, Houston, Texas, USA; Department of Oncology, Nanjing Hospital of Traditional Chinese Medicine, Nanjing, Jiangsu, China[e]

Ras can act on the plasma membrane (PM) to mediate extracellular signaling and tumorigenesis. To identify key components controlling Ras PM localization, we performed an unbiased screen to seek *Schizosaccharomyces pombe* mutants with reduced PM Ras. Five mutants were found with mutations affecting the same gene, *S. pombe erf2* (*sp-erf2*), encoding sp-Erf2, a palmitoyltransferase, with various activities. sp-Erf2 localizes to the *trans*-Golgi compartment, a process which is mediated by its third transmembrane domain and the Erf4 cofactor. In fission yeast, the human ortholog zDHHC9 rescues the phenotypes of *sp-erf2* null cells. In contrast, expressing zDHHC14, another sp-Erf2-like human protein, did not rescue Ras1 mislocalization in these cells. Importantly, *ZDHHC9* is widely overexpressed in cancers. Overexpressing *ZDHHC9* promotes, while repressing it diminishes, Ras PM localization and transformation of mammalian cells. These data strongly demonstrate that sp-Erf2/zDHHC9 palmitoylates Ras proteins in a highly selective manner in the *trans*-Golgi compartment to facilitate PM targeting via the *trans*-Golgi network, a role that is most certainly critical for Ras-driven tumorigenesis.

Mammals have three *RAS* genes, *HRAS*, *NRAS*, and *KRAS*, which encode membrane-bound GTPases that control a wide range of signal transduction pathways critical for growth, differentiation, and cytoskeleton remodeling (1). The best-known Ras function is to mediate growth factor signaling that occurs at the plasma membrane (PM), and deregulation of this and other Ras functions can promote tumor formation (2, 3). While all Ras proteins are farnesylated to gain general membrane affinity, a second signal is needed to specifically localize to the PM. For HRas and NRas, this signal is provided by palmitoylation at cysteine residues immediately upstream of the C-terminal CAAX motif. This reaction can be catalyzed by protein acyltransferases (PATs) that contain a DHHC domain rich with aspartate, histidine, and cysteine residues. These DHHC-PATs are expected to localize in the Golgi complex to allow the delivery of palmitoylated Ras proteins to the PM through the *trans*-Golgi system (4) although this concept has not been thoroughly demonstrated *in vivo*.

Humans have 24 DHHC-PATs, but it remains unresolved which of these control palmitoylation of Ras proteins *in vivo*. In contrast, the Ras pathways are considerably simpler in yeasts. Early studies from the budding yeast *Saccharomyces cerevisiae*, which has seven DHHC-PATs and two Ras proteins, suggest that only *S. cerevisiae* Erf2 (sc-Erf2) controls palmitoylation of its Ras proteins (5, 6). By sequence alignment to find putative orthologs, zDHHC9 was predicted to be a human Ras PAT (7). Although zDHHC9 can catalyze Ras palmitoylation *in vitro*, zDHHC9 cannot rescue *sc-erf2* mutant phenotypes in budding yeast (8), and until now there has been no evidence that zDHHC9 or other human DHHC-PATs can control Ras localization in mammalian cells. Furthermore, while ectopically expressed zDHHC9 localizes to the Golgi complex, sc-Erf2 appears mostly in the endoplasmic reticulum (ER). Therefore, the lack of cross-species conservation in how DHHC-PATs work between humans and budding yeast leaves open many unresolved questions.

In an unbiased approach to identify regulators of Ras trafficking to the PM, we mutagenized the fission yeast *Schizosaccharomyces pombe* to seek mutants whose Ras protein does not efficiently localize to the PM. *S. pombe* has a single Ras protein, Ras1, which controls two evolutionarily conserved pathways that are spatially segregated (9, 10). The Ras1–Byr2–mitogen-activated protein (MAP) kinase pathway (11) functions on the PM to mediate mating, while the Ras1-Scd1/Ral1-Cdc42 pathway (12, 13) functions in the endomembrane to mediate cell morphogenesis. We reasoned that reduced PM localization by Ras1 would result in sterility without affecting normal cell morphology. We isolated five mutants defective in the same gene, *S. pombe erf2* (*sp-erf2*), named due to its sequence similarity to sc-ERF2. sp-Erf2 is one of five fission yeast DHHC-PATs. We show here that it localizes to the *trans*- but not *cis*-Golgi compartment and is needed for Ras1 palmitoylation. Our sequence analysis also identified several human DHHC-PATs, including zDHHC9, that are highly related to sp-Erf2. Most importantly, ectopic expression of zDHHC9 but not the closely related protein zDHHC14 rescues all of the phenotypes of *sp-erf2*Δ cells. In human cells, zDHHC9 overexpression promotes, while *ZDHHC9* repression inhibits, Ras localization to the PM; furthermore, zDHHC9 is also both necessary and sufficient for Ras-induced oncogenic transformation. These results strongly suggest that sp-Erf2 is the most critical component in *S. pombe* that selectively palmitoylates Ras in the *trans*-Golgi compartment to allow efficient transport to the PM, such that even a

Received 23 September 2013 **Returned for modification** 16 October 2013
Accepted 9 November 2013
Published ahead of print 18 November 2013
Address correspondence to Eric C. Chang, echang1@bcm.edu.
Z.-Y.Z. and A.D.W. contributed equally to this article.
Supplemental material for this article may be found at http://dx.doi.org/10.1128/MCB.01248-13.

doi:10.1128/MCB.01248-13

partial loss of sp-Erf2 activity is sufficient to inactivate Ras signaling from the PM. Our data also unequivocally establishes zDHHC9 as a Ras PAT for mammalian cells, strongly suggesting that levels of zDHHC9 are tightly regulated to control Ras-induced tumorigenesis.

MATERIALS AND METHODS

Cells and growth conditions. The wild-type parental *S. pombe* strain is SP870 (*h*^{90} *ade6-210 leu1-32 ura4-D18*) (12). Transformations were performed by the lithium acetate method (14). Protoplast fusion was performed to facilitate complementation analysis of sterile strains. Strains that stably express green fluorescent protein (GFP)-Ras1 by the *ras1* promoter were described previously (10). A PCR-based method was used to delete *sp-erf2* by homologous recombination (15). To generate *ras1*Δ *sp-erf2*Δ cells, *sp-erf2* was deleted in *ras1*Δ cells (strain SPRN [11]) and confirmed by PCR. Multiple deletion clones were checked and were found to share the same phenotypes. The *erf4*$^{+/\Delta}$ strain was purchased from Bioneer Corporation (16). The rich medium (YEAU, consisting of yeast extract, dextrose, adenine, and uracil) and minimal medium (MM) were as described previously (17). For all experiments, cells were pregrown at 30°C to early log phase (≈0.4 × 10^7 to 1.0 × 10^7 cells/ml). To induce sexual differentiation, cells were shifted to MM lacking NH_4Cl and containing low glucose (18). To test for Ca^{2+} sensitivity, a sterile stock solution of 2 M $CaCl_2$ was added to rich medium after autoclaving. For spotting growth assays, cells were concentrated to an optical density at 600 nm (OD_{600}) of 1 to 2 and then serially diluted 1:5 in medium. To measure mating efficiency, colonies were patched onto MM plates, incubated at 28°C for 3 to 4 days, and then examined by microscopy to calculate the percentage of mated cells (asci plus zygotes). Vacuole staining was performed as follows. Cells were grown in rich medium to log phase, washed, and concentrated. A 16.3 mM stock solution of the lipophilic dye FM4-64 (Molecular Probes) was added to the cells (2 μl in 400 μl cells) for 30 min. The cells were washed with medium and then grown for an additional hour before imaging. Mammalian cell lines 293FT, HT1080, and NIH 3T3 were cultured as described previously (19). The acinus formation experiment of MCF10AT cells was conducted as described previously (20). The culture of MCF10AT and NIH 3T3 cells in soft agar was conducted as previously described (2, 20). SUM159 cells were cultured in F-12 medium supplemented with 5% fetal bovine serum (FBS), 5 μg/ml insulin, and 1 μg/ml hydrocortisone (Sigma). Transfection and virus production were generally performed as described previously (19). However, we found that high levels of zDHHC9 are toxic to many cells we used, including MCF10AT cells. To optimize the expression levels, we transduced the cells with serial doses of the virus and found that a multiplicity of infection (MOI) of 25 yielded desirable results while an MOI of ≥50 killed the cells.

Plasmids and plasmid construction. pRP-GFPRAS1, pRP-GFPRAS1G17V, pSLF173-RAS1, and pSLF173-RAS1G17V were as described previously (10). To truncate sp-Erf2 in the N terminus to delete the first 52 amino acids, pRES was digested by BamHI, and the resulting plasmid was religated after the overhang was filled in. The open reading frames (ORFs) of the *sp-erf2* genes from the mutants were amplified by PCR from genomic DNA and sequenced. For expression and localization studies, *sp-erf2* was amplified by PCR from the genomic DNA of strain SP870 and ligated into the BamHI sites of pARTCM, pSLF273, pREP81, and pREP41GFP (21). All PCR products in this study were validated by sequencing. pREP41-ERF2MC and pREP41-ERF2GFP were made by cloning the endogenously tagged *sp-erf2* by PCR from genomic DNA, digesting it with BglII and ligating it into the BamHI site of pREP41. pREP42-GMS1CFP was as described previously (22). Human *ZDHHC9* was amplified by PCR from clone HSCD00295927 (DNASU Plasmid Repository) (23), and *ZDHHC14* was cloned from human H9 embryonic stem cell cDNA; both were ligated into the BamHI site of pREP81. To express mCherry (MC)-tagged Ras in mammalian cells, wild-type *HRAS* and *NRAS* were amplified by PCR from cDNA. They were cloned into pENTR and then transferred to pCL/mCherry-DEST, yielding pCL/mCherry-HRas and pCL/mCherry-NRas, respectively. *ZDHHC9* was also transferred to pCL/GFP-DEST to construct pCL/GFP-ZDHHC9. The nonsilencing control and short hairpin RNAs (shRNAs) against *ZDHHC9* in the lentiviral pGIPZ vector were purchased from Open Biosystems. We screened five shRNAs and selected the two with the highest knockdown efficiency (from 5′ to 3′): CCGTATCAAGAATTTCCAGATA (clone 1) and CATGGAGATAGAAGCTACCAAT (clone 2).

Microscopy. The general method for imaging live *S. pombe* cells was as described previously (24) using an Olympus BX61 microscope with a 100×/1.3 (numerical aperture) UPlanFL oil immersion objective lens. Images were captured by a Hamamatsu ORCA ER digital camera. *Z*-stacks of yeast cells were collected at 0.25 to 0.5 μm for seven sections. Images used for quantification were deconvolved by constrained iteration in SlideBook (Intelligent Imaging Innovations). To measure the GFP-Ras1 distribution, we calculated the percentage of GFP intensity at the cell periphery with respect to the total GFP intensity in the cell from the central focal plane using the mask functions. The general method for imaging live mammalian cells by confocal microscopy was as described previously (19) using a Leica TCS SP5 confocal microscope with a 63×/1.4 oil immersion objective lens. To detect GFP and mCherry, we used 488-nm light with 30% of available argon laser power and 543-nm light with 80% of available He-Ne laser power. Images were analyzed using the LAS AF software (Leica) to calculate the portion of Ras at the PM over that in the whole cell (detailed in Fig. S1 in the supplemental material). To examine acini, an Olympus IX70 microscope with a 20×/0.4 LCPlan FL objective lens was used, and images were captured with a Retiga 1300 camera (QImaging) and processed in ImageJ.

Real-time reverse transcription-PCR (RT-PCR). Total RNAs were harvested using an RNeasy kit (Qiagen), and cDNAs were synthesized from 5 μg of total RNA using a SuperScript III First-Strand synthesis system (Life Technologies) according to the manufacturer's instructions. Real-time PCR was performed with Power SYBR green master mix on an ABI 7500 fast real-time PCR system (Life Technologies). The PCR primer pairs used were GTCTTCGCCTTCAACATCGT and AATCCAGTCAGT CCCACGAC (human *ZDHHC9*), GGAGGAAATGGGAGGTGTTC and TTCACCGCCAGGTACGGA (human *ZDHHC14*), GATTGGCTACCC AACTGTTGCA and CAGGGGCAGCAGCCACAAAGGC (human *36B4*), ATGGACAGGGAAGAATCGTG and TCCTCCAGTGGCAAAA TACC (mouse *Zdhhc9*), and GCACAGTCAAGGCCGAGAAT and GCC TTCTCCATGGTGGTGAA (mouse *Gapdh*). The relative amounts of PCR products generated from each primer set were determined on the basis of the threshold cycle (C_T).

Western blotting. GFP-Ras1 in the acyl-biotin exchange assay was probed with polyclonal GFP antibody (1:2,000; Invitrogen). The general methods and materials for detecting mammalian proteins by Western blotting were as described previously (19). All protein signals were measured by an Odyssey system using antibodies conjugated to fluorescent molecules (LiCOR). To detect zDHHC9, we screened several antibodies and found one from Sigma (1:500) that can strongly detect ectopically expressed zDHHC9. However, in most cell lines, endogenous zDHHC9 levels are low, and on Western blots, zDHHC9 is frequently masked by other proteins. We thus modified the SDS-PAGE system by changing the concentrations of both acrylamide and *bis*-acrylamide to allow better separation (25).

Mutagenesis screen. SP870 cells stably expressing GFP-Ras1 were cultured in YEAU medium to log phase and concentrated to 2 × 10^8 cells/ml in 0.1 M sodium phosphate buffer. Ethane methyl sulfonate (EMS) was added to the cells (50 μl in 0.2 ml) and incubated for 1 h at 30°C to yield a 60% kill rate. The treated cell suspension was transferred to a new tube containing 8 ml of 5% sodium thiosulfate to inactivate EMS and then spread on MM plates. After 5 days, ≈10^5 colonies were exposed to iodine vapor, which causes fertile cells to turn dark brown due to the presence of glycogen-rich spores. Approximately 2,000 white colonies were selected, and 7 of them were confirmed by microscopy as sterile (lack of spores)

with normal elongated cell morphology and with decreased GFP-Ras1 at the PM.

Genomic library screen. The *sp-erf2-1* mutant cells stably expressing GFP-Ras1 were transformed with 1 μg of a low-copy-number genomic library, pRSPL4.3 (26), and plated on YEAU plates. After overnight incubation, the cells were replica plated onto YEAU plates containing 100 mM $CaCl_2$, and 2 days later, cells were replica plated onto auxotrophic selective medium. Based on the transformation efficiency of the host cells (50,000 cells transformed) and the complexity of the library (10^6, or 2,100 genome equivalents), we expected that every *S. pombe* gene would be screened approximately 13 times. However, we isolated just one *S. pombe* colony that was reproducibly resistant to Ca^{2+}. The plasmid, named pRES by us, was isolated from cells in this colony.

Evolutionary trace analysis of sp-Erf2. The evolutionary trace (ET) was performed as described previously (27). The sp-Erf2 protein sequence was first blasted against the NCBI Reference Sequence database (28). In order to identify functional homologs, the protein sequences were filtered based on protein length (90% of the query protein) and sequence identity (>35%). We obtained 41 fungal homologs that were then aligned and analyzed (29). The identity of these homologous sequences and the analysis can all be found at http://mammoth.bcm.tmc.edu/aw11/erf2_analysis.html.

Sequence analysis of the DHHC-PAT family. The DHHC and transmembrane regions of sp-Erf2 were defined by the Uniprot resource (http://www.uniprot.org). Proteins were aligned using the PROMALS server (30). Sequence similarity was calculated with the BLOSUM62 matrix, and the phylogenetic tree was made with the unweighted pair group method with arithmetic mean (UPGMA).

Statistical analysis. All data are shown as means ± standard errors of the means (SEM). All *P* values were analyzed by an unpaired Student's *t* test compared to the wild type or vector control.

RESULTS

Isolation of *S. pombe* mutants with reduced *ras1* at the PM. To identify critical components that control Ras1 trafficking to the PM, we conducted a mutagenesis screen using *S. pombe* in which Ras1 controls two compartmentalized pathways with distinct and easily detectable signaling outputs (mating and elongated cell morphology). *S. pombe* cells stably expressing GFP-Ras1 were mutagenized by EMS (ethyl methanesulfonate) and first screened for sterility by an iodine vapor assay (31). Isolated colonies were then tested microscopically to confirm the presence of the normal elongated cell shape and the mislocalization of GFP-Ras1.

The mislocalization of GFP-Ras1 in five clones is apparent even during vegetative growth, with a substantial portion of GFP-Ras1 accumulated on internal membranous structures (Fig. 1A; see also Fig. S2A in the supplemental material) that resemble vacuoles. The Ras1-Byr2 mating pathway is tightly regulated spatially: Byr2 has been shown to translocate to the PM at the onset of sexual differentiation (32). Strikingly, when GFP-Ras1 was examined during sexual differentiation, it was essentially undetectable at the PM in all of the isolated mutants (Fig. 1A). Consistent with the concept that Ras1 PM localization is essential for mating, mating efficiencies in the mutants are substantially reduced (Fig. 1B; see also Fig. S2A). Further genetic tests showed that all five mutants carry recessive mutations and belong to the same complementation group, indicating that the same gene was identified five times in our screen.

The mutated gene encodes the palmitoyltransferase Erf2. In microscopy experiments, we noticed that the vacuoles in the isolated mutants are about half the diameter of those in the parental cells (see Fig. S2B in the supplemental material). Such a phenotype may reflect defects in the vacuole protein sorting or vesicle trafficking and often coincides with sensitivity to high Ca^{2+} levels

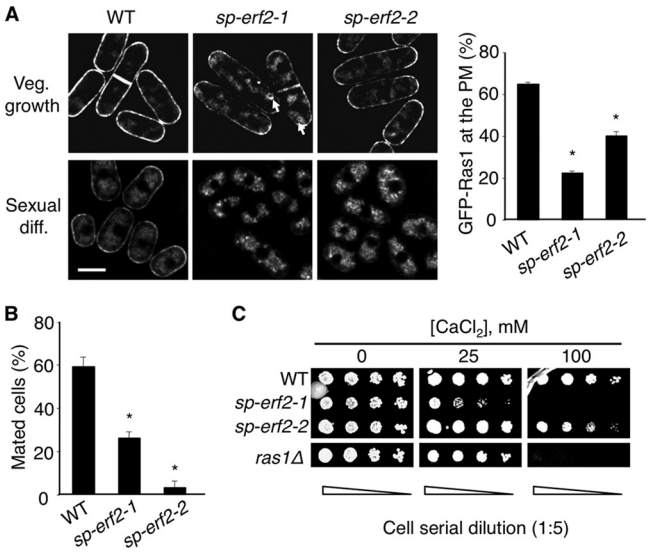

FIG 1 Phenotype of *sp-erf2* mutants. (A) Wild-type (WT) cells and two examples of strains carrying mutant alleles of *sp-erf2* expressing GFP-Ras1 (stably transformed by pRP-GFPRAS1) were either grown in rich medium to log phase or starved in nitrogen-depleted minimal medium to induce sexual differentiation, and their GFP-Ras1 was examined by deconvolution fluorescence microscopy. For vegetative cells, the percentage of GFP-Ras1 at the PM versus the whole cell for the central focal plane of individual cells was quantified as shown on the right ($n = 20$ cells; *, $P < 10^{-15}$). The arrows point to circular structures that resemble vacuoles. We note that in budding yeast mutants where Ras is mislocalized from the plasma membrane, Ras also accumulated on the vacuole (5) Scale bar, 10 μm. (B) Mating efficiency was calculated after patching colonies on MM plates. At least 500 cells were counted for each colony patch ($n = 3$ colonies; *, $P < 0.007$). (C) Cells were grown to log phase and serially diluted and spotted on plates with the indicated amounts of $CaCl_2$.

(33). We thus screened the isolated mutants and found that four of them are hypersensitive to Ca^{2+} (Fig. 1C; see also Fig. S2A). This robust Ca^{2+} sensitivity enabled us to identify the wild-type version of the gene in these mutants by complementation. To this end, we chose the mutant with the strongest Ca^{2+} phenotype as host, which was transformed with a low-copy-number genomic library (1 to 2 plasmids/cell) (see Materials and Methods) and plated in the presence of high levels of Ca^{2+}. We recovered one library clone carrying two full-length genes. By deletion analysis, we determined that only *erf2* was needed to rescue the phenotype of the mutant cells.

The *erf2* gene in *S. pombe* was first identified as *mug142* (*m*eiosis *u*pregulated) because it is induced during meiosis (34, 35). Erf2 is named after the putative ortholog *ERF2* in *S. cerevisiae*, which is a palmitoyltransferase (36), and recently *S. pombe* Erf2 has been shown to regulate the palmitoylation of Ras (37). To distinguish between the *erf2* in *S. pombe* and that in *S. cerevisiae*, we have added a prefix (*sp* or *sc*, respectively). We named the mutant allele in the strain used for the complementation screen *sp-erf2-1*. Indeed, when *sp-erf2* was deleted in the parental strain (*sp-erf2*Δ), *sp-erf2*Δ cells induced the same phenotypes as the *sp-erf2-1* strain (see Fig. S2 in the supplemental material), and they are allelic by genetic segregation analysis (data not shown). These data collectively suggest that we isolated mutations of *sp-erf2* in our screen, and we named these mutants *sp-erf2-1-5*.

Despite the presence of five closely related DHHC-PATs in *S. pombe*, mutants defective in *sp-erf2* were the only DHHC-PAT

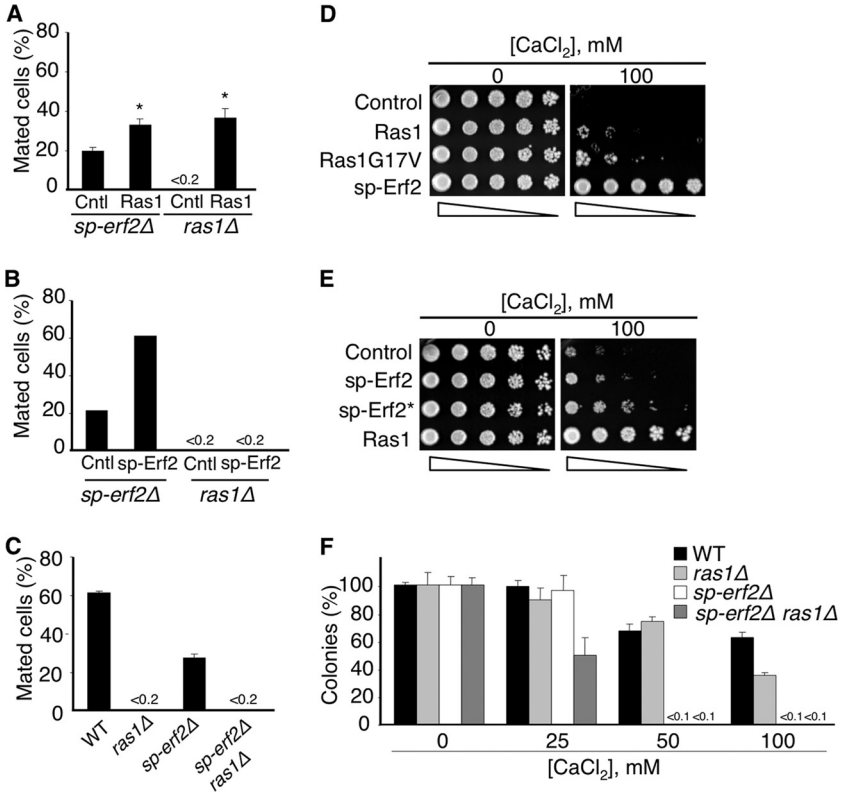

FIG 2 Epistatic analysis of *sp-erf2* and *ras1* cells. (A) *sp-erf2*Δ and *ras1*Δ cells were transformed with either a vector control (Cntl) or linearized pRP-GFPRAS1, which expresses GFP-tagged Ras1, using a *ras1* promoter. Cells in which GFP-Ras1 was stably expressed were selected. Mating was examined in $n \geq 4$ patches, and in each patch, >500 cells were examined, resulting in a detection limit of 0.2% (*, $P = 0.005$). (B) *sp-erf2*Δ and *ras1*Δ cells were transformed with a vector control or with pSLF273-ERF2. Colonies were pooled, and the mating efficiency was measured. We note that the mating efficiency of wild-type cells in our hands is about 60%. While sp-Erf2 overexpression in *sp-erf2*Δ cells fully restored mating to wild-type levels, Ras1 overexpression in *ras1*Δ cells did not. We believe that this is due to too much Ras1 activity, which can inhibit the mating response (65, 66). (C) Cells ($n = 3$ patches) of the indicated genotype were induced to mate, and the mating efficiency was calculated as described for panel A. (D) *sp-erf2*Δ cells were transformed with the vector control or with a vector expressing wild-type Ras1 (pSLF173-RAS1), constitutively active Ras1 (pSLF173-RAS1G17V), or Erf2 (pSLF273-ERF2). Transformed cells were serially diluted and spotted on plates with the indicated levels of added $CaCl_2$. (E) *ras1*Δ cells were transformed either with the vector control or with pSLF273-ERF2 or pARTCM-ERF2, which express Erf2 by the relatively weak *nmt1* promoter or the strong *adh* promoter (marked by an asterisk). Since *adh-erf2* is toxic to cells grown in liquid, transformants directly from the plate were used for spotting. To overexpress Ras1, pSLF173-RAS1 was used, and the resulting cells were examined as described for panel D. (F) Approximately 1,000 logarithmically grown cells of the indicated genotype were spread in triplicate ($n = 3$) on plates with different concentrations of Ca^{2+}, resulting in a detection limit of 0.1%. The emerged colonies were counted, and the colony numbers were normalized to those of the no-Ca^{2+} control.

mutants we isolated, and they were isolated five times. Furthermore, GFP-Ras1 was not detectably mislocalized when genes encoding other nonessential DHHC-PATs were deleted (see Fig. S3 in the supplemental material). These results strongly suggest that *sp-erf2* encodes the primary DHHC-PAT controlling Ras1 PM localization.

Epistasis analysis on the relationship between sp-Erf2 and Ras1. To determine whether sp-Erf2 and Ras1 act in the same pathway and in what order they act, we performed genetic experiments using null mutants. Since sp-Erf2 is proposed to control Ras1 localization to the PM, we first examined how sp-Erf2 interacts with Ras1 with respect to mating. When *ras1* was overexpressed in *sp-erf2*Δ cells, the mating efficiency of *sp-erf2*Δ cells was increased (Fig. 2A); conversely, when *sp-erf2* was overexpressed in *ras1*Δ cells, the sterility of *ras1*Δ cells was not affected (Fig. 2B). In addition, when both *ras1* and *sp-erf2* were deleted, the double mutant was viable and as sterile as *ras1*Δ cells (Fig. 2C). These data agree with the model that Erf2 acts upstream of Ras1 in a linear pathway for mating. Intriguingly, cells defective in Ras1 and sp-Erf2 are both hypersensitive to Ca^{2+}. When either wild-type or constitutively active Ras1 was overexpressed, the Ca^{2+} tolerance in *sp-erf2*Δ cells was improved (Fig. 2D); reciprocally, when *sp-erf2* was overexpressed, Ca^{2+} tolerance was improved in *ras1*Δ cells (Fig. 2E). Furthermore, *ras1*Δ *sp-erf2*Δ cells are viable although their Ca^{2+} sensitivity is stronger than that of cells in the single mutants (Fig. 2F). These data support the possibility that with respect to Ca^{2+} tolerance, Ras1 and sp-Erf2 act cooperatively.

Protein sequence analysis of sp-Erf2 and related proteins to predict functional domains and human orthologs. We analyzed the amino acid sequence of sp-Erf2 in order to define functional domains necessary for controlling Ras activity. sp-Erf2 is predicted to have four transmembrane domains (TMDs), with both the N and C termini, as well as an inner loop containing a conserved DHHC domain, facing the cytoplasm (Fig. 3A). To establish the general evolutionary importance of these residues, we applied the evolutionary trace (ET) method (29, 38), which uses phylogenetic relationships in related proteins to estimate the relative evolutionary pressure on each residue. Evolutionarily important residues identified by ET have been shown to coincide with functional sites within proteins (39–41). As shown in Fig. 3B,

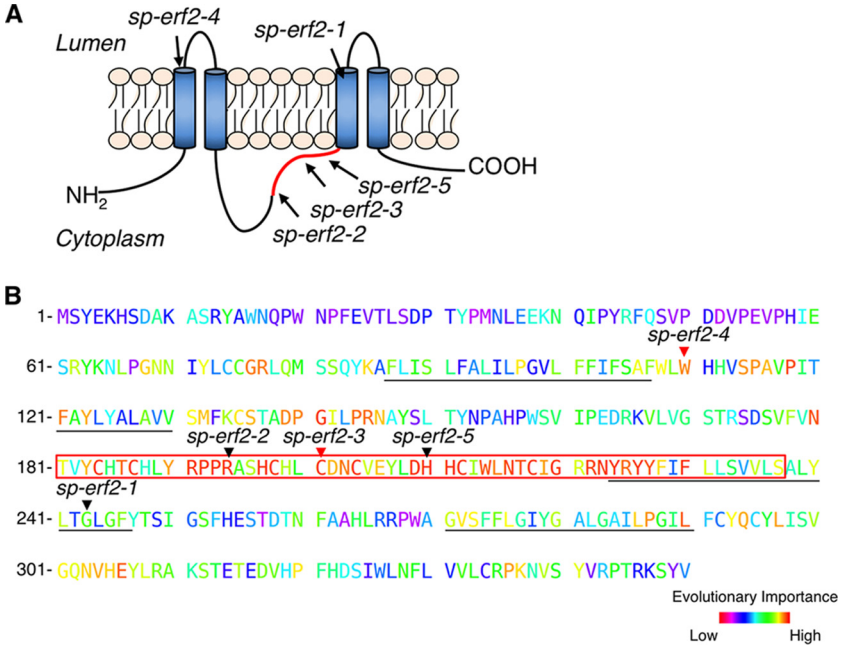

FIG 3 Protein sequence analysis of sp-Erf2. (A) Putative sp-Erf2 topology predicted by TMRPres2D software (67) utilizing the hydrophobicity plot prediction algorithm TMHMM, version 2.0. Arrows mark the regions of the protein affected by the mutagenesis in the screen. (B) The degree of variation for a given residue in sp-Erf2 is shown in a color-coded evolutionary trace heat map, where the residues shown in red are the most evolutionarily important while those in purple are the least important. Predicted transmembrane regions are underlined. The DHHC motif is boxed in red. Arrowheads mark residues mutated in the screen; in particular, red arrowheads denote mutations that yield a truncation product.

the first 60 or so amino acids were found to have low evolutionary importance and contain no obvious protein sequence motifs. In addition, during the course of the deletion analysis on pRES, we created a truncated sp-Erf2 lacking the first 52 amino acids (Materials and Methods) and found that it was functionally indistinguishable from wild-type sp-Erf2. These results suggest that the first 60 residues are not functionally critical.

The most evolutionarily important region is from amino acid residue 190 to 230 (Fig. 3B), a region which contains the DHHC domain, a hallmark of PATs. Studies of sc-Erf2 confirm that the DHHC residues, such as H201, are directly involved in the palmitoylation reaction (42). We sequenced the *sp-erf2* ORF in each of the mutants (Fig. 3B), and in support of the concept that H201 is critical to Ras palmitoylation, replacing the corresponding residue in sp-Erf2 (H210) with tyrosine (encoded by *sp-erf2-5*) created a nearly null phenotype (Fig. S2A see Fig. S2A in the supplemental material). The arginine at position 194 is conserved among homologs, and even a substitution with another positively charged amino acid histidine, encoded by *sp-erf2-2*, generated a readily detectable phenotype. Finally, the *sp-erf2-3* mutation produces an early stop codon at position 201, leading to the loss of half of the DHHC domain and the rest of sp-Erf2 and, not surprisingly, yielding a null-like phenotype. These and other results support the concept that the DHHC region is essential for the catalytic activity of sp-Erf2 and other PATs.

Of the TMDs, the two TMDs in the C terminus are moderately more evolutionarily important than the two in the N terminus (Fig. 3B), suggesting that the latter TMDs may be more important for the function of PATs. In support of this, our genetic data indicate that the *sp-erf2-1* mutation results in a glycine-to-arginine substitution at position 243 and produces the most severe phenotype even though the DHHC region is intact. In contrast, *erf2-4* introduces an early stop codon at position 110 within the first TMD to cause one of the mildest phenotypes (Fig. 1; see also Fig. S2A in the supplemental material). We suspect that the *erf2-4* mutant protein starts at a second methionine at position 132 to produce a truncated protein with an intact DHHC region and two C-terminal TMDs but lacking the first two TMDs. In conclusion, our data suggest that while the DHHC region is essential for the catalytic activity for Erf2 and other PATs, the C-terminal TMDs are also essential for the biological functions of these proteins, perhaps by controlling where the protein localizes and interacts with substrates.

sp-Erf2 controls Ras1 palmitoylation and localizes to the *trans*-Golgi compartment. Since proteins with the DHHC domain are predicted to be PATs, we measured levels of Ras1 palmitoylation in the cell by an acyl-biotin exchange assay (43). Consistent with the model that sp-Erf2 catalyzes Ras1 palmitoylation, GFP-Ras1 labeled by *N*-[6-(biotinamido)hexyl]-3-(2′-pyridyldithio)propionamide (biotin-HPDP) and pulled down by streptavidin in *sp-erf2*Δcells is greatly reduced, suggesting that it is not efficiently palmitoylated (Fig. 4A).

Based on current models of protein palmitoylation in mammalian cells, a Ras PAT would be expected to reside in the Golgi complex (4, 7). To examine this in *S. pombe*, we first attempted to tag endogenous sp-Erf2 by various fluorescent proteins (in single or triple copy) via homologous recombination. However, sp-Erf2 appeared to be expressed at very low levels and was undetectable despite our efforts to induce it by nitrogen starvation (data not shown). We thus subcloned the genomically C-terminally tagged sp-Erf2 and ectopically expressed it by a moderate thiamine-repressible *nmt* (*nmt***) promoter. We also similarly expressed sp-

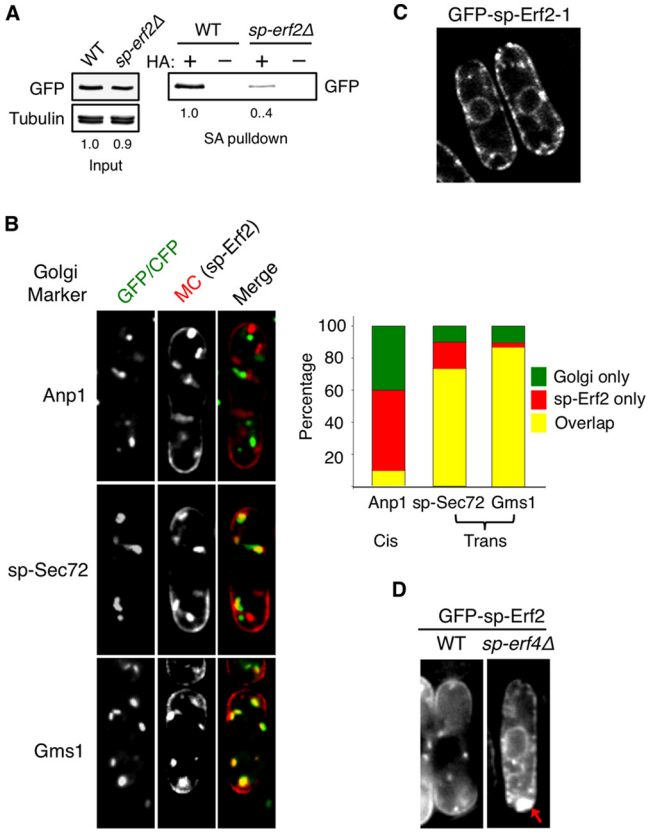

FIG 4 Sp-Erf2 is required for efficient Ras1 palmitoylation and localizes to the *trans*-Golgi compartment. (A) Lysates from wild-type and *sp-erf2*Δ cells expressing GFP-Ras1 were first incubated in *N*-ethylmaleimide to cap all free cysteines (nonpalmitoylated). Lysates were treated with hydroxylamine (HA; +) or with a Tris buffer as control (−) to remove palmitoyl groups. Newly exposed cysteines could then be tagged by biotin-HPDP, which is pulled down with streptavidin (SA) and detected by Western blotting. (B) Cells carrying Anp1-GFP or sp-Sec72–GFP were transformed by pREP41-ERF2MC, which expresses MC-tagged Erf2; in addition, SP870 cells were cotransformed with vectors expressing Gms1-cyan fluorescent protein (CFP) and Erf2-MC (by pREP42-GMS1CFP and pREP41-ERF2MC). These cells were grown in MM and then examined by deconvolution fluorescence microscopy. There are approximately 5 to 7 dots each of sp-Erf2–MC and a Golgi marker in the central plane of a given cell (left). The percent overlap between sp-Erf2 dots and Golgi marker dots in a cell ($n > 200$ dots in at least 20 cells) was quantified as shown on the right. (C) *sp-erf2*Δ cells were transformed with a vector expressing the GFP-tagged mutant Erf2-1 (using pREP41-GFPERF2-1) and examined as described for panel B. (D) *sp-erf4*$^{+}$ (WT) and *sp-erf4*Δ cells, derived from the same *sp-erf4*$^{+/\Delta}$ diploid cell, were transformed to express GFP–sp-Erf2 (pREP41-GFPERF2) and examined by fluorescence microscopy. An arrow marks *sp-erf4*Δ cells containing apparent GFP–sp-Erf2 aggregates.

Erf2 tagged at the N terminus. In both cases, tagged sp-Erf2 rescued the phenotypes of *sp-erf2*Δ cells as efficiently as the untagged version (see Fig. S4A in the supplemental material). These results indicate that the tagged versions of sp-Erf2 can be used as good surrogates for further studying sp-Erf2 localization. By microscopy, N- or C-terminally tagged sp-Erf2–GFP can be readily seen at the cell tips and as mobile dots (Fig. 4B and data not shown), which resemble Golgi markers. A similar conclusion has been reached from a previous study that globally examined subcellular localization of *S. pombe* proteins (44).

To further examine whether these mobile dots are indeed Golgi markers, we treated the tagged cells with brefeldin A (BFA), which is known to also collapse the Golgi complex into the endoplasmic reticulum (ER) in *S. pombe* (45). Our data showed that the GFP–sp-Erf2 dots in the BFA-treated cells were no longer visible, and more GFP–sp-Erf2 could be seen colocalizing with an ER marker (24) encircling the nucleus (see Fig. S4B in the supplemental material). To decipher in which Golgi compartments sp-Erf2 localizes, we examined markers for two key Golgi compartments, Anp1 for the *cis*-Golgi compartment (46) and sp-Sec72 and Gms1 for the *trans*-Golgi compartment (22, 46, 47). Vesicles are received from the ER by the *cis*-Golgi compartment and can be delivered to the PM from the *trans*-Golgi compartment. Our data showed that sp-Erf2 did not markedly colocalize with the *cis*-Golgi marker although they were often adjacent to one another (Fig. 4B). In contrast, substantial overlap was observed between sp-Erf2 and either of the *trans*-Golgi markers. These data strongly support the model that Ras palmitoylation by sp-Erf2 occurs primarily in the *trans*-Golgi compartment to allow efficient delivery to the PM.

Our sequence analysis (Fig. 3B) suggests that the *sp-erf2-1* mutation (G243R) can interfere with the interaction between its third TMD and cell membranes. In support of this, our data show that GFP–sp-Erf2-1 localizes primarily to the ER, as evident by the characteristic signal at the nuclear ring, cytoplasmic tubules, and cell periphery (Fig. 4C). It has been shown that sc-Erf2 appears to work together with a nonenzymatic cofactor, sc-Erf4 (48), whose *in vivo* role remains largely unclear. *S. pombe* has a putative sp-Erf4 ortholog. We found that its loss creates growth defects not seen with the *sp-erf2*Δ cells, which may be why it was not isolated in the initial mutagenesis screen (see Discussion). In *sp-erf4*Δ cells, Ras1 localization to the PM was diminished (see Fig. S3 in the supplemental material). Importantly, we also examined GFP-Erf2 in *sp-erf4*Δ cells and found that GFP-Erf2 appeared to form large aggregates, and its localization to the Golgi complex was reduced with an increase in ER localization, as seen with the sp-Erf2-1 mutant (Fig. 4D). These data strongly suggest that Golgi localization is essential for sp-Erf2 regulation of Ras1, and this process requires G243 in its third TMD and a functional Erf4.

zDHHC9 controls PM localization of Ras proteins in *S. pombe*. There are 24 DHHC-PATs in humans. To predict which would be the closest putative orthologs to sp-Erf2, we first aligned the 5 fission yeast, 7 budding yeast, and 24 human DHHC-PATs. This whole sequence comparison readily separated sp-Erf2 from the four other *S. pombe* DHHC-PATs and from the majority of human DHHC-PATs (Table 1) but did not lead to a clear evolutionary kinship with a human ortholog. Next, we focused on the sequence similarity among the most important functional residues, as predicted by an evolutionary trace of sp-Erf2. Consistent with the findings of other groups (7, 49), we found that in the most functionally relevant parts of the sequence, zDHHC9 was the most similar to sp-Erf2, earmarking it as a potential Ras PAT for human cells. Strikingly, we found that sp-Erf2 is more similar to zDHHC9 than it is to sc-Erf2 in functional residues.

zDHHC9 has also been suggested to be a Ras PAT in biochemical assays using purified proteins (7); however, there is no data to show that *in vivo* zDHHC9 acts as a Ras PAT. Notably, zDHHC9 could not rescue the phenotype of budding yeast *sc-erf2*Δ cells (8), and repressing it in human cells did not affect HRas localization (4). Regardless, we investigated whether human zDHHC9 can replace sp-Erf2 in *S. pombe*. Remarkably, when zDHHC9 was expressed in *sp-erf2*Δ cells, Ca^{2+} tolerance, Ras1 PM localization, and mating were all readily restored (Fig. 5). In contrast, when the

TABLE 1 Protein sequence similarity of a subset of DHHC-PATs to sp-Erf2

Protein[a]	Percent similarity of the indicated region or sequence to sp-Erf2[b]			
	Whole sequence	DHHC alone	DHHC+TMD	Top 50% residues
zDHHC9	32	82	55	54
zDHHC14	33	78	50	51
zDHHC18	31	75	50	49
zDHHC5	25	77	50	45
zDHHC8	25	78	49	45
zDHHC19	26	61	42	38
sc-Erf2	33	71	51	49

[a] After whole protein sequences were analyzed, this subset of human DHHC-PATs and sc-Erf2 were readily separated from the rest of the DHHC-PATs in humans, budding yeast, and fission yeast to be closely related to sp-Erf2.
[b] To further determine which human DHHC-PATs are most closely related to sp-Erf2, regions of high conservation were analyzed. We analyzed either just the DHHC domain, the DHHC domain together with the TMDs, or the top 50% ranked amino acid residues as determined by ET.

closely related zDHHC14 (Table 1) was expressed, only Ca^{2+} sensitivity was rescued (see Fig. S5 in the supplemental material). These results strongly support the model that zDHHC9 specifically regulates Ras functions.

zDHHC9 controls PM localization of Ras proteins in human cells. To functionally validate the role of zDHHC9 on Ras in human cells, we measured Ras localization to the PM when zDHHC9 was either repressed (by gene silencing) or overexpressed. We chose the human fibrosarcoma HT1080 cell line for the gene silencing experiments in part because these cells have a spread-out cell morphology ideal for comparing Ras levels at the PM and cytoplasm. We screened shRNA clones by quantitative PCR (qPCR) and found two that efficiently and selectively repressed *ZDHHC9* expression but not that of the closely related *ZDHHC14* (data not shown). To optimize the gene-silencing experiments, we performed both qPCR and Western blotting at two time points (7 and 14 days) after gene silencing. As shown in Fig. 6A, although *ZDHHC9* mRNA levels were already greatly reduced at day 7, a 50 to 60% reduction in zDHHC9 protein levels was not observed until day 14. The shRNA did not affect levels of endogenous NRas, which is overexpressed in this cell line, glyceraldehyde-3-phosphate dehydrogenase (GAPDH), or total extracellular signal-regulated kinase (ERK), but it did reduce phospho-Erk1/2 levels, a marker of Ras signaling (Fig. 6B).

We then went on to examine the effect of *ZDHHC9* repression on Ras localization using mCherry (MC)-tagged NRas as a reporter. HT1080 cells selected for carrying the shRNA vector were transfected at day 6 and day 13 to express MC-NRas, and the resulting cells were examined 24 h later live by confocal microscopy. In agreement with the time course of zDHHC9 protein reduction after gene silencing, *ZDHHC9* knockdown caused a ~50% reduction in PM MC-NRas, concomitant with an increase of MC-NRas in the cytoplasm, at day 14 (Fig. 6C) but not at day 7 (see Fig. S6 in the supplemental material). This effect was abrogated by a cDNA encoding zDHHC9 that is refractory to the shRNA, further demonstrating that zDHHC9 is specifically responsible for proper Ras localization to the PM. HRas was also tested and yielded similar results (see Fig. S7).

Conversely, we investigated whether zDHHC9 overexpression can induce Ras localization to the PM. For this study, we chose to focus on NRas because it is frequently found in the cytoplasm at higher levels than HRas, presumably due to the fact that NRas has one palmitolylation site whereas HRas has two (50). This phenomenon is evident in SUM159 human breast cancer cells (Fig. 6D). We expressed either GFP-zDHHC9 or the GFP vector control, together with MC-NRas, and found that zDHHC9 overexpression doubled NRas at the PM as examined by confocal microscopy. In addition, NRas and zDHHC9 signals overlap substantially in these cells in a perinuclear region, supporting the concept that they can interact in the Golgi complex.

zDHHC9 controls Ras-induced transformation. Ras proteins are well known drivers for many types of cancers, but until now, the key way to gauge their impacts on cancer was to measure oncogenic mutations. It is conceivable that factors such as zDHHC9 that can increase Ras signaling outputs on the PM can

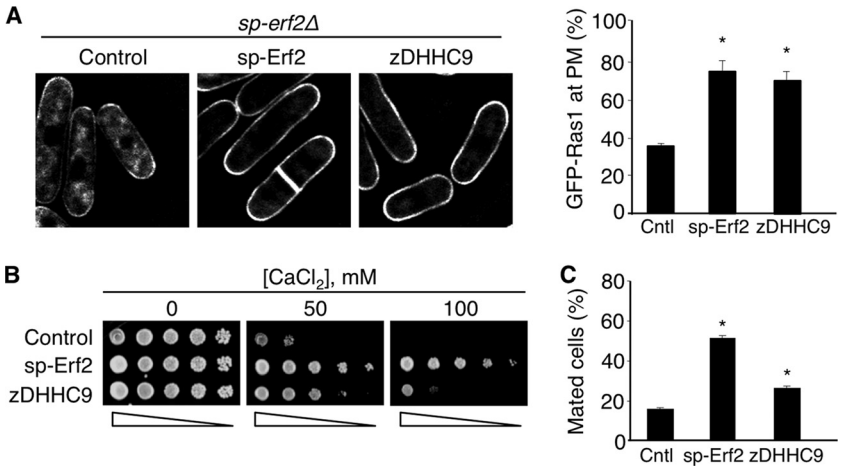

FIG 5 zDHHC9 can replace sp-Erf2 in *S. pombe* and control Ras1 localization. (A) *sp-erf2*Δ cells stably expressing GFP-Ras1 were transformed either with a vector control or with a vector expressing sp-Erf2 (pREP81-ERF2) or zDHHC9 (pREP81-ZDHHC9) and examined by microscopy as described in the legend of Fig. 1A ($n = 15$ cells; *, $P < 10^{-4}$). (B) Cells from the experiment shown in panel A were tested for Ca^{2+} sensitivity as described in the legend of Fig. 1C. (C) Cells from the experiment shown in panel A were tested for mating in triplicate ($n = 3$) as described in the legend of Fig. 1B. *, $P \leq 0.01$.

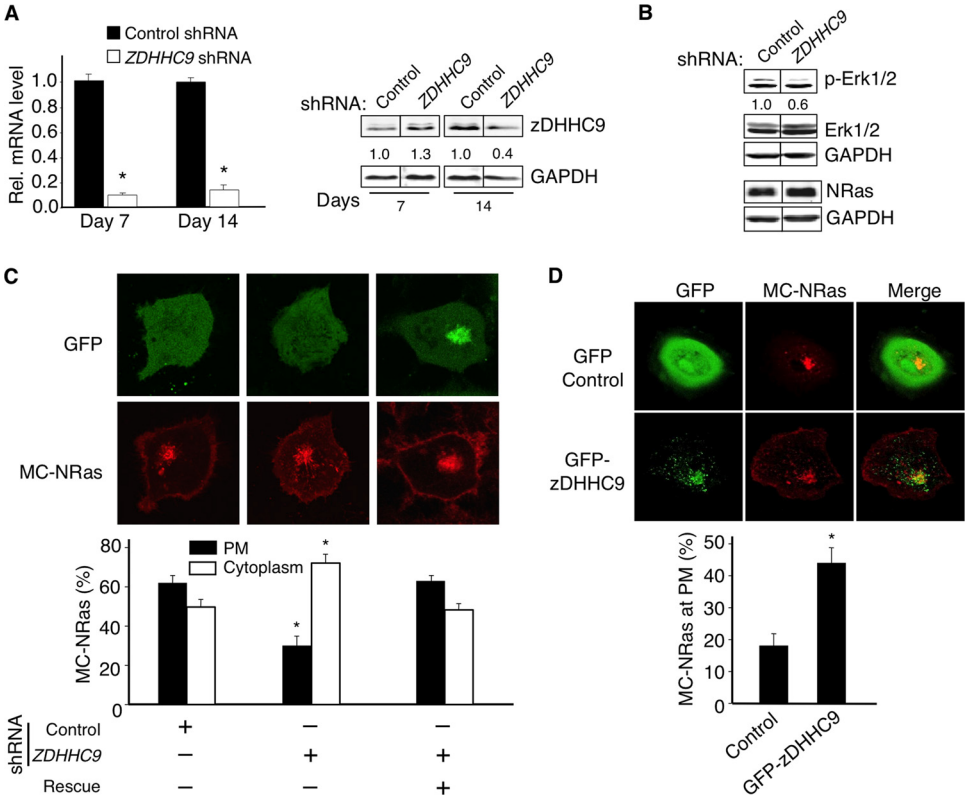

FIG 6 zDHHC9 is both necessary and sufficient to control Ras PM localization in mammalian cells. (A) HT1080 cells were transduced by a puromycin-selectable viral vector that expresses either a control or shRNA against *ZDHHC9* (clone 2). The cells were grown in puromycin and examined by qPCR on day 7 and 14 ($n = 3$ reactions; *, $P < 0.05$). Similar results were obtained with another shRNA clone (clone 1) (data not shown). For the rest of the studies using human cells, clone 2 shRNA was used throughout. To determine knockdown efficiencies at the protein level, HT1080 cells were similarly silenced, and the lysates were examined by Western blotting. Relative zDHHC9 levels, normalized to GAPDH, are shown below the blot. (B) *ZDHHC9* in HT1080 cells was similarly silenced as described for panel A, and 14 days after transduction, the indicated proteins were examined by Western blotting. Relative phospho-Erk1/2 levels, normalized to GAPDH, are shown below the blot. (C) *ZDHHC9* in HT1080 cells was repressed as described for panel A. On day 13, cells were transfected to express MC-NRas, and the *ZDHHC9*-repressed cells were also transfected with or without shRNA-refractory GFP-zDHHC9 (Rescue). They were examined the next day by confocal microscopy. We note that the shRNA vector is marked by GFP, whose signal is diffused in the cell. In contrast, GFP-zDHHC9 mostly appears in the endomembrane compartment. Therefore, for the rescue we analyzed MC-NRas in cells with the appropriate GFP patterns. The relative levels of MC-NRas at the PM and cytoplasm were quantified. Cell numbers were as follows: 32 for control shRNA, 22 for *ZDHHC9* shRNA, and 11 for *ZDHHC9* shRNA plus Rescue (*, $P < 0.01$). (D) SUM159 cells were cotransfected to express MC-NRas, together with either a GFP vector control or GFP-zDHHC9, and examined by microscopy as described for panel C ($n = 7$ cells, vector control; $n = 10$ cells, GFP-zDHHC9) (*, $P < 0.05$).

also promote tumor formation. Indeed, zDHHC9 has been shown to be upregulated in colorectal cancer (51) by immunohistochemistry. To further examine the scale of zDHHC9 overexpression in cancers, we searched the Oncomine database, which has a large collection of gene expression studies from a wide range of cancers. As shown in Fig. 7A, we detected *ZDHHC9* overexpression in many additional cancers. As a comparison, we also searched *SOS1* and *SOS2* (*SOS1/2*) which encode guanine nucleotide exchange factors, the best known of Ras activators, and found that they are only sparsely overexpressed in human cancers and that there seem to be as many cancers in which they are downregulated. This observation suggests that among known proteins that directly regulate Ras, overexpression of *ZDHHC9* but not *SOS1/2* appears to be favorably selected for during tumor formation in a wide range of tissues.

To ascertain whether zDHHC9 can modulate Ras-induced transformation, we first turned to a classic model of cellular transformation using murine NIH 3T3 cells. We have generated NIH 3T3 cells that stably express oncogenic HRas with a Q61L mutation [HRas(Q61L)] or KRas-4B(Q61L) (2, 19). PM Ras proteins in these cells are known to signal to the Raf-Erk MAP kinase pathway, which is important for cell transformation. As shown in Fig. 7B, *Zdhhc9* silencing reduced Erk phosphorylation induced by oncogenic HRas but not by oncogenic KRas-4B, which is not palmitoylated. NIH 3T3 cells expressing HRas(Q61L) can efficiently form colonies in soft agar, bypassing anchorage dependence. However, when *Zdhhc9* was repressed, the number of colonies that emerged was reduced by half (Fig. 7C). We note that a similar reduction in colony formation was obtained when the palmitoylation sites in HRas(Q61L) were mutated (Fig. 7C), creating HRas(Q61L C181S C184S) which transforms cells by activating only cytoplasmic effectors (2, 52–54). In further support of the concept that repression of *Zdhhc9* selectively blocks Ras signaling at the PM, we found that *Zdhhc9* knockdown did not inhibit colony formation in NIH 3T3 cells expressing the palmitoylation-deficient HRas(Q61L C181S C184S).

ZDHHC9 overexpression can be found in cancers that frequently harbor oncogenic *RAS* mutations, such as colon cancer, as

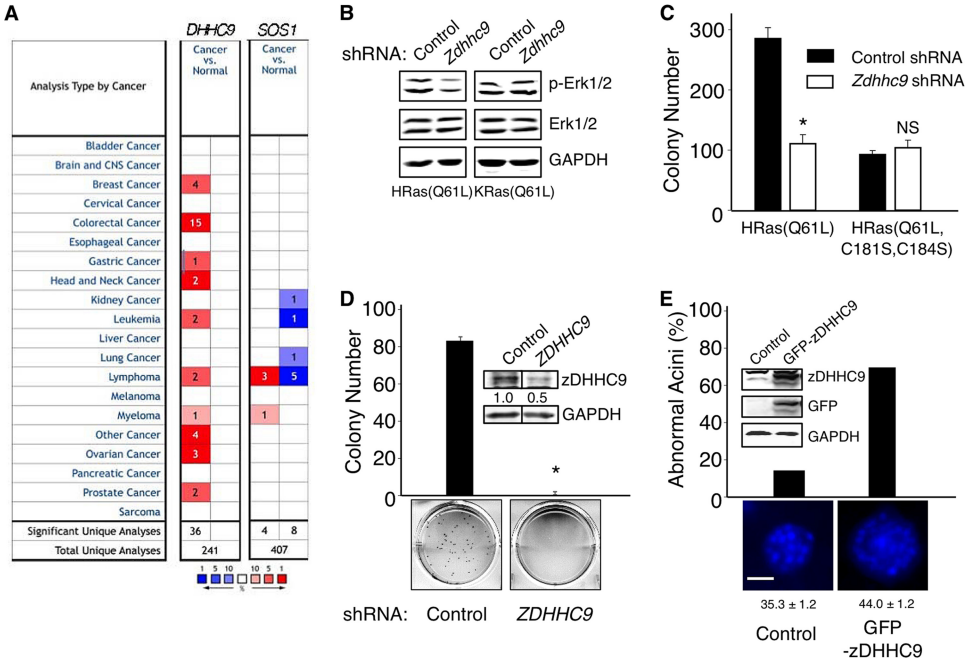

FIG 7 zDHHC9 controls Ras-induced mammalian cell transformation. (A) Gene summary from Oncomine search. The search thresholds were as follows: 1.5-fold change, *P* value of $<10^{-4}$, and gene rank of <10%. Overexpression is marked by red, while repression is marked by blue. The number in the cell indicates the number of studies meeting the search thresholds. The color intensity map (bottom) corresponds to the best gene rank percentile; e.g., a deep red means that it is ranked at the top 1% most overexpressed. (B) NIH 3T3 cells stably expressing HRas(Q61L) or KRas-4B(Q61L) were infected with the shRNA *ZDHHC9* clone 1, which is better matched with mouse *Zdhhc9* sequence, and cultured for 14 days with puromycin. Cells were lysed, and the indicated proteins were examined by Western blotting. (C) NIH 3T3 cells stably expressing HRas(Q61L) or palmitoylation-deficient HRas(Q61L C181S C184S) were infected with shRNA and grown in puromycin for 14 days before being seeded in soft agar in triplicate ($n = 3$). *, $P < 0.01$; NS, not significant. (D) *ZDHHC9* in MCF10AT cells was silenced by shRNA as described for panel C, and lysates were examined by Western blotting. Similarly prepared cells were seeded for colony formation in soft agar. *, $P < 0.01$. (E) MCF10AT cells were transfected to express a control GFP vector or GFP-zDHHC9 and cultured with puromycin for 4 to 5 days. Lysates were examined by Western blotting. Transfected cells were seeded into Matrigel and cultured for 13 days to form acini. The nuclei of cells in acini were stained with Hoechst 33342 and examined by microscopy, as shown below the graph. Scale bar, 20 μm. The diameter (μm) of acini was measured in ImageJ, and the value is shown below the photograph (for the control, $n = 29$ acini; for GFP-zDHHC9, $n = 65$ acini; *, $P < 0.005$). Abnormal acini are defined as acini that are greater than the mean diameter of control acini plus 1 standard deviation (6.5 μm).

well as in cancers not previously known to contain frequent *RAS* mutations, such as prostate and breast cancers (Fig. 7A) (55). For example, we analyzed microarray data of human breast tumors from The Cancer Genome Atlas (TCGA) (56) and found that *ZDHHC9* levels are 2-fold higher in tumors than in normal tissues (see Fig. S8A in the supplemental material). Moreover, *ZDHHC9* levels are particularly elevated in two breast cancer subtypes (57), basal-like and Her2$^+$ (see Fig. S8B), known to be dependent on growth factor signaling for growth. To investigate the role of zDHHC9 in human breast cancer, we used a premalignant breast cancer cell line, MCF10AT, which was derived from the normal basal-like human mammary epithelial MCF10A line after oncogenic HRas was introduced (58). While the parental MCF10A cells cannot form colonies in soft agar, MCF10AT cells can do so modestly. However, when *ZDHHC9* was repressed, colony formation was abolished (Fig. 7D). In three-dimensional culture using Matrigel, mammary epithelial cells can form acini, ball-like structures that resemble terminal end buds in the mammary gland. Proper acinus formation is sensitive to oncogenic activity, such as hyperproliferation, which can increase acinus size (20, 59). To test whether zDHHC9 can promote tumorigenic properties, we overexpressed GFP-zDHHC9 in MCF10AT cells and seeded the cells in Matrigel. As shown in Fig. 7E, zDHHC9 overexpression led to a 4-fold increase in acini that are abnormally large compared to cells expressing the vector control. All together, we have demonstrated definitively that zDHHC9 is a key factor controlling Ras localization to the PM, as well as Ras-induced transformation in mammalian cells.

DISCUSSION

While Ras proteins must localize to the PM to mediate extracellular signaling, how Ras PM targeting is controlled remains incompletely understood. Guided by the *S. pombe* sp-Erf2–Ras1 pathway uncovered in this study, the data strongly support the model that zDHHC9 acts as a Ras PAT in the *trans*-Golgi compartment, enabling palmitoylated Ras proteins to be readily delivered to the PM. Most importantly, *ZDHHC9* is more widely overexpressed in human cancers than *SOS1/2*; in addition, we demonstrate that *ZDHHC9* repression inhibits, while *ZDHHC9* overexpression promotes, Ras-induced transformation. Therefore, it seems highly probable that *ZDHHC9* overexpression is favorably selected to promote tumorigenesis.

Our results differ from previous studies of sc-Erf2 and zDHHC9 in several ways that may reveal how DHHC-PATs control Ras in other eukaryotes. The first major difference is that human zDHHC9 cannot rescue the phenotype of budding yeast *sc-erf2* mutant cells (8), while zDHHC9 can fully rescue the *sp-erf2*Δ phenotype in *S. pombe*. We speculate that this difference

may be explained by the possibility that Ras palmitoylation is cell compartment specific (see below): sc-Erf2 is mainly localized to the ER but not the Golgi complex, where the bulk of sp-Erf2 and zDHHC9 reside. We found that the Golgi localization of sp-Erf2 requires a glycine at position 243 in the third TMD, and replacing this glycine with a negatively charged residue disrupts it. Interestingly, the corresponding position of G243 in zDHHC9 is an alanine, which structurally and chemically resembles glycine; in contrast, it is a threonine in sc-Erf2. These results suggest that proper Golgi localization requires that a position corresponding to 243 must be an amino acid with a very short side chain that cannot interact with its neighboring residues by charge or hydrogen bonding. It is also possible that zDHHC9 cannot interact with budding yeast Ras proteins because they are structurally different from those in humans and *S. pombe*. For example, Ras proteins structurally diverge most substantially in the C-terminal region known as the hypervariable region (HVR). Among known Ras proteins, budding yeast Ras proteins have the longest HVR, with 117 amino acid residues that must be trimmed off in order to function in mammalian cells (59). In contrast, *S. pombe* Ras1 is much closer to human Ras proteins in terms of HVR length (47 versus 24 amino acids).

sc-Erf2 has been shown to work together with sc-Erf4 although the *in vivo* function of sc-Erf4 is not fully understood. Our data indicate that in *sp-erf4*Δ cells, sp-Erf2 is prone to aggregate formation and mislocalizes from the Golgi complex. We thus propose that sp-Erf4 is needed for proper sp-Erf2 folding and localization. While sp-Erf2 is mislocalized to the ER in the *sp-erf2-1* mutant, it does not form aggregates as it does in *sp-erf4*Δ cells. Therefore, mislocalization to the ER, in and of itself, does not induce sp-Erf2 aggregate formation. Finally, we speculate that sp-Erf2 aggregates may be targeted by the protein quality control system, which may explain why in budding yeast, loss of sc-Erf4 induces polyubiquitylation on sc-Erf2 (60). In the initial budding yeast screen, several *sc-erf4* mutations were isolated (5); in this screen, however, *sp-erf4* mutations were not isolated. We believe that in *S. pombe* at least, sp-Erf4 can control functions not shared with sp-Erf2 that are important for proper cell growth. For example, in our attempt to select *sp-erf4*$^{+}$ and *sp-erf4*Δ haploid cells from an *sp-erf4*$^{+/\Delta}$ diploid, the *sp-erf4*Δ cells appeared at a frequency of just 8%, far less than expected (50%), and the transformed *sp-erf4*Δ cells also emerged much more slowly (data not shown). In further support of the concept that *sp-erf4* can control a different set of functions, in a recent global analysis of synthetic genetic interactions in *S. pombe* using null mutants (61), while *sp-erf4* and *sp-erf2* interacted with a common set of genes, they also interacted with different genes.

Rocks et al. have previously repressed expression of zDHHC9 in HeLa cells and reported that this did not affect the localization of tagged HRas, which led to the conclusion that DHHC-PATs in human cells are functionally redundant (4). They examined *ZDHHC9* mRNA levels after knockdown, and it is possible that Ras localization was examined just a few days after knockdown, which is how this type of experiment is routinely conducted. Based on our data, however, substantial reduction of zDHHC9 protein levels could take up to 14 days after gene silencing; therefore, the zDHHC9 protein is apparently long-lived. In turn, we strongly argue that protein palmitoylation is performed by PATs with a high level of selectivity. First, unbiased genetic screens in both budding yeast and fission yeast identified only one DHHC-PAT, Erf2, multiple times as a Ras regulator. Follow-up studies have shown that deleting other PATs, either singularly or in combination, does not affect Ras (6) (see Fig. S3 in the supplemental material). Thus, at least in both *S. pombe* and *S. cerevisiae*, separated by up to a billion years of evolution (62), the interactions between their Erf2 and Ras proteins are highly selective. In mammals, we observed a good correlation between the degree of selective reduction of zDHHC9 protein levels and Ras mislocalization from the PM. Furthermore, while zDHHC14 is among those human PATs that are closely related to sp-Erf2 and zDHHC9, it could restore only Ca^{2+} tolerance and not Ras1 PM localization in *S. pombe*. While the interaction between Ras proteins and a given PAT is selective, some Ras proteins in *sc-erf2*Δ budding yeast, as well as in vegetatively growing *sp-erf2*Δ fission yeast cells, can still be seen at the PM. We believe that this pool of Ras protein is covalently modified since a Ras1 mutant lacking the cysteine for palmitoylation (C215S) could not be seen at the PM at all (10). It has been shown that palmitoylation can be driven by acyl coenzyme A (CoA) concentration *in vitro* without PATs (63, 64), so we support the idea that this cysteine in Ras proteins could be spontaneously modified to gain PM affinity.

How DHHC-PATs recognize substrates with selectivity is an important question but beyond the scope of this study. We can offer a few ideas, however, with respect to Ras signaling. Since sp-Erf2 localization to *trans*-Golgi compartment is critical for Ras control, we speculate that the interaction between a PAT and its substrate could be spatially compartmentalized in the cell. Furthermore, the expression of sp-Erf2 (and perhaps that of human zDHHC9) is tightly regulated. sp-Erf2 is expressed at very low levels and not detectable by genomic epitope tagging, yet it is induced during meiosis. When the levels of sp-Erf2 are substantially elevated during meiosis, it can selectively increase the palmitoylation of another substrate, Rho3, in a dose-dependent manner (37). We found that when either sp-Erf2 or zDHHC9 was ectopically overexpressed in yeast by the strong *adh* promoter, it was toxic, and cells grew poorly. Therefore, substrate selectivity can also be maintained by tightly controlling PAT protein levels. sp-Erf2 has other substrates, which may be responsible for proper growth at high levels of Ca^{2+}. One of the mutants isolated from the screen, the *sp-erf2-2* mutant, is defective in Ras1 PM localization but not in Ca^{2+} tolerance. The *sp-erf2-2* mutation affects a conserved residue within the DHHC region; thus, it is possible that this region has the intrinsic ability to differentiate one substrate from another.

To assess the impact of Ras signaling pathways on cancer, current approaches almost exclusively center on detecting oncogenic mutations in the *RAS* genes. By this approach alone, impressively, approximately 30% of all human cancers contain such *RAS* mutations. However, we suggest that when *ZDHHC9* overexpression is factored in, the actual impact of Ras on cancer is likely to be much greater. For example, our data suggest that signaling activities from wild-type Ras proteins at the PM are also important for the development of many cancers, such as breast cancer, in which oncogenic *RAS* mutations are rare. Furthermore, even in cancers in which oncogenic *RAS* mutations are frequent, knowing the status of zDHHC9 levels may more precisely define which Ras proteins are involved in promoting tumor formation. For example, colon cancers are among the cancers in which *ZDHHC9* is most frequently overexpressed. Despite this, approximately 50% of colon cancers have *KRAS* mutations, and KRas-4B is thought to

be the main culprit for inducing tumorigenesis. Since KRas-4B as shown here is not dependent on zDHHC9 for proper functioning, it is possible that other zDHHC9-dependent Ras proteins (e.g., KRas-4A, NRas, and HRas) also play a key role in promoting colon cancers. In contrast, *ZDHHC9* overexpression is absent in pancreatic cancers, over 90% of which contain oncogenic *KRAS*. One interpretation of this observation is that in pancreatic cancers, KRas-4B is the lone driver for tumorigenesis. However, we caution that zDHHC9 overexpression alone may not be sufficient to induce tumor formation because this can be toxic to the cells. Thus, zDHHC9 overexpression may need to work in conjunction with additional genetic alterations to efficiently induce tumorigenesis.

ACKNOWLEDGMENTS

We thank Wayne P. Wahls (University of Arkansas for Medical Sciences), Sara Mole (University College London), and Snezhana Oliferenko (Temasek Lifesciences Lab) for kindly providing reagents and Charles M. Perou and Cheng Fan (University of North Carolina) for help in analyzing microarray data.

We also sincerely thank our funding sources. A Graduate Research Fellowship from the National Science Foundation supported E.Y. Z.-Y.Z. was supported by a postdoctoral fellowship from the Susan G. Komen for the Cure Foundation (PDF0707860). The Jiangsu Health International Exchange Program sponsored M.L. E.C.C. is supported by grants from the NIH (CA90464, CA107187, GM81627, P30-CA58183, and CA125123), the Nancy Owens Memorial Foundation, and the Mary Kay Ash Foundation. O.L. is supported by grants from the NIH (R01-GM066099, R01-GM079656) and NSF (ABI-1062455).

REFERENCES

1. **Ahearn IM, Haigis K, Bar-Sagi D, Philips MR.** 2012. Regulating the regulator: post-translational modification of RAS. Nat. Rev. Mol. Cell. Biol. **13:**39–51. http://dx.doi.org/10.1038/nrm3255.
2. **Cheng CM, Li H, Gasman S, Huang J, Schiff R, Chang EC.** 2011. Compartmentalized Ras proteins transform NIH 3T3 cells with different efficiencies. Mol. Cell. Biol. **31:**983–997. http://dx.doi.org/10.1128/MCB.00137-10.
3. **Cuiffo B, Ren R.** 2010. Palmitoylation of oncogenic NRAS is essential for leukemogenesis. Blood **115:**3598–3605. http://dx.doi.org/10.1182/blood-2009-03-213876.
4. **Rocks O, Gerauer M, Vartak N, Koch S, Huang ZP, Pechlivanis M, Kuhlmann J, Brunsveld L, Chandra A, Ellinger B, Waldmann H, Bastiaens PI.** 2010. The palmitoylation machinery is a spatially organizing system for peripheral membrane proteins. Cell **141:**458–471. http://dx.doi.org/10.1016/j.cell.2010.04.007.
5. **Bartels DJ, Mitchell DA, Dong X, Deschenes RJ.** 1999. Erf2, a novel gene product that affects the localization and palmitoylation of Ras2 in *Saccharomyces cerevisiae*. Mol. Cell. Biol. **19:**6775–6787.
6. **Roth AF, Wan J, Bailey AO, Sun B, Kuchar JA, Green WN, Phinney BS, Yates JR, III, Davis NG.** 2006. Global analysis of protein palmitoylation in yeast. Cell **125:**1003–1013. http://dx.doi.org/10.1016/j.cell.2006.03.042.
7. **Swarthout JT, Lobo S, Farh L, Croke MR, Greentree WK, Deschenes RJ, Linder ME.** 2005. DHHC9 and GCP16 constitute a human protein fatty acyltransferase with specificity for H- and N-Ras. J. Biol. Chem. **280:**31141–31148. http://dx.doi.org/10.1074/jbc.M504113200.
8. **Mitchell DA, Vasudevan A, Linder ME, Deschenes RJ.** 2006. Protein palmitoylation by a family of DHHC protein S-acyltransferases. J. Lipid Res. **47:**1118–1127. http://dx.doi.org/10.1194/jlr.R600007-JLR200.
9. **Chang EC, Philips MR.** 2006. Spatial segregation of Ras signaling: new evidence from fission yeast. Cell Cycle **5:**1936–1939. http://dx.doi.org/10.4161/cc.5.17.3187.
10. **Onken B, Wiener H, Philips MR, Chang EC.** 2006. Compartmentalized signaling of Ras in fission yeast. Proc. Natl. Acad. Sci. U. S. A. **103:**9045–9050. http://dx.doi.org/10.1073/pnas.0603318103.
11. **Wang Y, Xu HP, Riggs M, Rodgers L, Wigler M.** 1991. *byr2*, a *Schizosaccharomyces pombe* gene encoding a protein kinase capable of partial suppression of the ras1 mutant phenotype. Mol. Cell. Biol. **11:**3554–3563.
12. **Chang EC, Barr M, Wang Y, Jung V, Xu HP, Wigler MH.** 1994. Cooperative interaction of S. pombe proteins required for mating and morphogenesis. Cell **79:**131–141. http://dx.doi.org/10.1016/0092-8674(94)90406-5.
13. **Fukui Y, Yamamoto M.** 1988. Isolation and characterization of *Schizosaccharomyces pombe* mutants phenotypically similar to *ras1*. Mol. Gen. Genet. **215:**26–31. http://dx.doi.org/10.1007/BF00331298.
14. **Suga M, Hatakeyama T.** 2005. A rapid and simple procedure for high-efficiency lithium acetate transformation of cryopreserved *Schizosaccharomyces pombe* cells. Yeast **22:**799–804. http://dx.doi.org/10.1002/yea.1247.
15. **Janke C, Magiera MM, Rathfelder N, Taxis C, Reber S, Maekawa H, Moreno-Borchart A, Doenges G, Schwob E, Schiebel E, Knop M.** 2004. A versatile toolbox for PCR-based tagging of yeast genes: new fluorescent proteins, more markers and promoter substitution cassettes. Yeast **21:**947–962. http://dx.doi.org/10.1002/yea.1142.
16. **Kim DU, Hayles J, Kim D, Wood V, Park HO, Won M, Yoo HS, Duhig T, Nam M, Palmer G, Han S, Jeffery L, Baek ST, Lee H, Shim YS, Lee M, Kim L, Heo KS, Noh EJ, Lee AR, Jang YJ, Chung KS, Choi SJ, Park JY, Park Y, Kim HM, Park SK, Park HJ, Kang EJ, Kim HB, Kang HS, Park HM, Kim K, Song K, Song KB, Nurse P, Hoe KL.** 2010. Analysis of a genome-wide set of gene deletions in the fission yeast *Schizosaccharomyces pombe*. Nat. Biotechnol. **28:**617–623. http://dx.doi.org/10.1038/nbt.1628.
17. **Alfa CE, Gallagher IM, Hyams JS.** 1993. Antigen localization in fission yeast. Methods Cell Biol. **37:**201–222. http://dx.doi.org/10.1016/S0091-679X(08)60251-4.
18. **Mata J, Wilbrey A, Bahler J.** 2007. Transcriptional regulatory network for sexual differentiation in fission yeast. Genome Biol. **8:**R217. http://dx.doi.org/10.1186/gb-2007-8-10-r217.
19. **Zheng ZY, Cheng CM, Fu XR, Chen LY, Xu L, Terrillon S, Wong ST, Bar-Sagi D, Songyang Z, Chang EC.** 2012. CHMP6 and VPS4A mediate the recycling of Ras to the plasma membrane to promote growth factor signaling. Oncogene **31:**4630–4638. http://dx.doi.org/10.1038/onc.2011.607.
20. **Suo J, Snider SJ, Mills GB, Creighton CJ, Chen AC, Schiff R, Lloyd RE, Chang EC.** 2011. Int6 regulates both proteasomal degradation and translation initiation and is critical for proper formation of acini by human mammary epithelium. Oncogene **30:**724–736. http://dx.doi.org/10.1038/onc.2010.445.
21. **Forsburg SL, Sherman DA.** 1997. General purpose tagging vectors for fission yeast. Gene **191:**191–195. http://dx.doi.org/10.1016/S0378-1119(97)00058-9.
22. **Codlin S, Mole SE.** 2009. *S. pombe btn1*, the orthologue of the Batten disease gene CLN3, is required for vacuole protein sorting of Cpy1p and Golgi exit of Vps10p. J. Cell Sci. **122:**1163–1173. http://dx.doi.org/10.1242/jcs.038323.
23. **Cormier CY, Park JG, Fiacco M, Steel J, Hunter P, Kramer J, Singla R, LaBaer J.** 2011. PSI:Biology-materials repository: a biologist's resource for protein expression plasmids. J. Struct. Funct. Genomics **12:**55–62. http://dx.doi.org/10.1007/s10969-011-9100-8.
24. **Otero JH, Suo J, Gordon C, Chang EC.** 2010. Int6 and Moe1 interact with Cdc48 to regulate ERAD and proper chromosome segregation. Cell Cycle **9:**147–161. http://dx.doi.org/10.4161/cc.9.1.10312.
25. **Anderson CW, Baum PR, Gesteland RF.** 1973. Processing of adenovirus 2-induced proteins. J. Virol. **12:**241–252.
26. **Wahls WP, Davidson MK.** 2008. Low-copy episomal vector pFY20 and high-saturation coverage genomic libraries for the fission yeast *Schizosaccharomyces pombe*. Yeast **25:**643–650. http://dx.doi.org/10.1002/yea.1605.
27. **Wilkins A, Erdin S, Lua R, Lichtarge O.** 2012. Evolutionary trace for prediction and redesign of protein functional sites. Methods Mol. Biol. **819:**29–42. http://dx.doi.org/10.1007/978-1-61779-465-0_3.
28. **Pruitt KD, Tatusova T, Klimke W, Maglott DR.** 2009. NCBI Reference Sequences: current status, policy and new initiatives. Nucleic Acids Res. **37:**D32–36. http://dx.doi.org/10.1093/nar/gkn721.
29. **Mihalek I, Res Lichtarge IO.** 2004. A family of evolution-entropy hybrid methods for ranking protein residues by importance. J. Mol. Biol. **336:**1265–1282. http://dx.doi.org/10.1016/j.jmb.2003.12.078.
30. **Pei J, Kim BH, Tang M, Grishin NV.** 2007. PROMALS web server for accurate multiple protein sequence alignments. Nucleic Acids Res. **35:**W649–652. http://dx.doi.org/10.1093/nar/gkm227.
31. **Moreno S, Klar A, Nurse P.** 1991. Molecular genetic analysis of fission

yeast *Schizosaccharomyces pombe*. Methods Enzymol. **194:**795–823. http://dx.doi.org/10.1016/0076-6879(91)94059-L.
32. **Bauman P, Cheng QC, Albright CF.** 1998. The Byr2 kinase translocates to the plasma membrane in a Ras1-dependent manner. Biochem. Biophys. Res. Commun. **244:**468–474. http://dx.doi.org/10.1006/bbrc.1998.8292.
33. **Iwaki T, Osawa F, Onishi M, Koga T, Fujita Y, Hosomi A, Tanaka N, Fukui Y, Takegawa K.** 2003. Characterization of *vps33*$^{+}$, a gene required for vacuolar biogenesis and protein sorting in *Schizosaccharomyces pombe*. Yeast **20:**845–855. http://dx.doi.org/10.1002/yea.1011.
34. **Martin-Castellanos C, Blanco M, Rozalen AE, Perez-Hidalgo L, Garcia AI, Conde F, Mata J, Ellermeier C, Davis L, San-Segundo P, Smith GR, Moreno S.** 2005. A large-scale screen in *S. pombe* identifies seven novel genes required for critical meiotic events. Curr. Biol. **15:**2056–2062. http://dx.doi.org/10.1016/j.cub.2005.10.038.
35. **Mata J, Lyne R, Burns G, Bahler J.** 2002. The transcriptional program of meiosis and sporulation in fission yeast. Nat. Genet. **32:**143–147. http://dx.doi.org/10.1038/ng951.
36. **Lobo S, Greentree WK, Linder ME, Deschenes RJ.** 2002. Identification of a Ras palmitoyltransferase in *Saccharomyces cerevisiae*. J. Biol. Chem. **277:**41268–41273. http://dx.doi.org/10.1074/jbc.M206573200.
37. **Zhang MM, Wu PY, Kelly FD, Nurse P, Hang HC.** 2013. Quantitative control of protein *S*-palmitoylation regulates meiotic entry in fission yeast. PLoS Biol. **11:**e1001597. http://dx.doi.org/10.1371/journal.pbio.1001597.
38. **Lichtarge O, Bourne HR, Cohen FE.** 1996. An evolutionary trace method defines binding surfaces common to protein families. J. Mol. Biol. **257:**342–358. http://dx.doi.org/10.1006/jmbi.1996.0167.
39. **Adikesavan AK, Katsonis P, Marciano DC, Lua R, Herman C, Lichtarge O.** 2011. Separation of recombination and SOS response in *Escherichia coli* RecA suggests LexA interaction sites. PLoS Genet. **7:**e1002244. http://dx.doi.org/10.1371/journal.pgen.1002244.
40. **Ribes-Zamora A, Mihalek I, Lichtarge O, Bertuch AA.** 2007. Distinct faces of the Ku heterodimer mediate DNA repair and telomeric functions. Nat. Struct. Mol. Biol. **14:**301–307. http://dx.doi.org/10.1038/nsmb1214.
41. **Rodriguez GJ, Yao R, Lichtarge O, Wensel TG.** 2010. Evolution-guided discovery and recoding of allosteric pathway specificity determinants in psychoactive bioamine receptors. Proc. Natl. Acad. Sci. U. S. A. **107:**7787–7792. http://dx.doi.org/10.1073/pnas.0914877107.
42. **Mitchell DA, Mitchell G, Ling Y, Budde C, Deschenes RJ.** 2010. Mutational analysis of *Saccharomyces cerevisiae* Erf2 reveals a two-step reaction mechanism for protein palmitoylation by DHHC enzymes. J. Biol. Chem. **285:**38104–38114. http://dx.doi.org/10.1074/jbc.M110.169102.
43. **Wan J, Roth AF, Bailey AO, Davis NG.** 2007. Palmitoylated proteins: purification and identification. Nat. Protoc. **2:**1573–1584. http://dx.doi.org/10.1038/nprot.2007.225.
44. **Matsuyama A, Arai R, Yashiroda Y, Shirai A, Kamata A, Sekido S, Kobayashi Y, Hashimoto A, Hamamoto M, Hiraoka Y, Horinouchi S, Yoshida M.** 2006. ORFeome cloning and global analysis of protein localization in the fission yeast *Schizosaccharomyces pombe*. Nat. Biotechnol. **24:**841–847. http://dx.doi.org/10.1038/nbt1222.
45. **Turi TG, Webster P, Rose JK.** 1994. Brefeldin A sensitivity and resistance in *Schizosaccharomyces pombe*. Isolation of multiple genes conferring resistance. J. Biol. Chem. **269:**24229–24236.
46. **Vjestica A, Tang XZ, Oliferenko S.** 2008. The actomyosin ring recruits early secretory compartments to the division site in fission yeast. Mol. Biol. Cell **19:**1125–1138. http://dx.doi.org/10.1091/mbc.E07-07-0663.
47. **Iwaki T, Hosomi A, Tokudomi S, Kusunoki Y, Fujita Y, Giga-Hama Y, Tanaka N, Takegawa K.** 2006. Vacuolar protein sorting receptor in *Schizosaccharomyces pombe*. Microbiology **152:**1523–1532. http://dx.doi.org/10.1099/mic.0.28627-0.
48. **Zhao L, Lobo S, Dong X, Ault AD, Deschenes RJ.** 2002. Erf4p and Erf2p form an endoplasmic reticulum-associated complex involved in the plasma membrane localization of yeast Ras proteins. J. Biol. Chem. **277:**49352–49359. http://dx.doi.org/10.1074/jbc.M209760200.
49. **Ohno Y, Kihara A, Sano T, Igarashi Y.** 2006. Intracellular localization and tissue-specific distribution of human and yeast DHHC cysteine-rich domain-containing proteins. Biochim. Biophys. Acta **1761:**474–483. http://dx.doi.org/10.1016/j.bbalip.2006.03.010.
50. **Choy E, Chiu VK, Silletti J, Feoktistov M, Morimoto T, Michaelson D, Ivanov IE, Philips MR.** 1999. Endomembrane trafficking of ras: the CAAX motif targets proteins to the ER and Golgi. Cell **98:**69–80. http://dx.doi.org/10.1016/S0092-8674(00)80607-8.
51. **Mansilla F, Birkenkamp-Demtroder K, Kruhoffer M, Sorensen FB, Andersen CL, Laiho P, Aaltonen LA, Verspaget HW, Orntoft TF.** 2007. Differential expression of DHHC9 in microsatellite stable and instable human colorectal cancer subgroups. Br. J. Cancer **96:**1896–1903. http://dx.doi.org/10.1038/sj.bjc.6603818.
52. **Cheng CM, Chang EC.** 2011. Busy traveling Ras. Cell Cycle **10:**1180–1181. http://dx.doi.org/10.4161/cc.10.8.15259.
53. **Chiu VK, Bivona T, Hach A, Sajous JB, Silletti J, Wiener H, Johnson RL, II, Cox AD, Philips MR.** 2002. Ras signalling on the endoplasmic reticulum and the Golgi. Nat. Cell Biol. **4:**343–350. http://dx.doi.org/10.1038/ncb783.
54. **Hancock JF, Magee AI, Childs JE, Marshall CJ.** 1989. All ras proteins are polyisoprenylated but only some are palmitoylated. Cell **57:**1167–1177. http://dx.doi.org/10.1016/0092-8674(89)90054-8.
55. **Bos JL.** 1989. *ras* oncogenes in human cancer: a review. Cancer Res. **49:**4682–4689.
56. **Koboldt DC, Fulton RS, McLellan MD, Schmidt H, Kalicki-Veizer J, McMichael JF, Fulton LL, Dooling DJ, Ding L, Mardis ER, Wilson RK, Ally A, Balasundaram M, Butterfield YS, Carlsen R, Carter C, Chu A, Chuah E, Chun HJ, Coope RJ, Dhalla N, Guin R, Hirst C, Hirst M, Holt RA, Lee D, Li HI, Mayo M, Moore RA, Mungall AJ, Pleasance E, Robertson A, Schein JE, Shafiei A, Sipahimalani P, Slobodan JR, Stoll D, Tam A, Thiessen N, Varhol RJ, Wye N, Zeng T, Zhao Y, Birol I, Jones SJ, Marra MA, Cherniack AD, Saksena G, Onofrio RC, Pho NH, et al. The Cancer Genome Atlas Network.** 2012. Comprehensive molecular portraits of human breast tumours. Nature **490:**61–70. http://dx.doi.org/10.1038/nature11412.
57. **Curtis C, Shah SP, Chin SF, Turashvili G, Rueda OM, Dunning MJ, Speed D, Lynch AG, Samarajiwa S, Yuan Y, Graf S, Ha G, Haffari G, Bashashati A, Russell R, McKinney S, Langerod A, Green A, Provenzano E, Wishart G, Pinder S, Watson P, Markowetz F, Murphy L, Ellis I, Purushotham A, Borresen-Dale AL, Brenton JD, Tavare S, Caldas C, Aparicio S.** 2012. The genomic and transcriptomic architecture of 2,000 breast tumours reveals novel subgroups. Nature **486:**346–352. http://dx.doi.org/10.1038/nature10983.
58. **Dawson PJ, Wolman SR, Tait L, Heppner GH, Miller FR.** 1996. MCF10AT: a model for the evolution of cancer from proliferative breast disease. Am. J. Pathol. **148:**313–319.
59. **Debnath J, Muthuswamy SK, Brugge JS.** 2003. Morphogenesis and oncogenesis of MCF-10A mammary epithelial acini grown in three-dimensional basement membrane cultures. Methods **30:**256–268. http://dx.doi.org/10.1016/S1046-2023(03)00032-X.
60. **Mitchell DA, Hamel LD, Ishizuka K, Mitchell G, Schaefer LM, Deschenes RJ.** 2012. The Erf4 subunit of the yeast Ras palmitoyl acyltransferase is required for stability of the acyl-Erf2 intermediate and palmitoyl transfer to a Ras2 substrate. J. Biol. Chem. **287:**34337–34348. http://dx.doi.org/10.1074/jbc.M112.379297.
61. **Frost A, Elgort MG, Brandman O, Ives C, Collins SR, Miller-Vedam L, Weibezahn J, Hein MY, Poser I, Mann M, Hyman AA, Weissman JS.** 2012. Functional repurposing revealed by comparing S. pombe and S. cerevisiae genetic interactions. Cell **149:**1339–1352. http://dx.doi.org/10.1016/j.cell.2012.04.028.
62. **Heckman DS, Geiser DM, Eidell BR, Stauffer RL, Kardos NL, Hedges SB.** 2001. Molecular evidence for the early colonization of land by fungi and plants. Science **293:**1129–1133. http://dx.doi.org/10.1126/science.1061457.
63. **Bano MC, Jackson CS, Magee AI.** 1998. Pseudo-enzymatic S-acylation of a myristoylated yes protein tyrosine kinase peptide in vitro may reflect non-enzymatic S-acylation in vivo. Biochem. J. **330:**723–731.
64. **Linder ME, Deschenes RJ.** 2007. Palmitoylation: policing protein stability and traffic. Nat. Rev. Mol. Cell Biol. **8:**74–84. http://dx.doi.org/10.1038/nrm2084.
65. **Nadin-Davis SA, Nasim A, Beach D.** 1986. Involvement of ras in sexual differentiation but not in growth control in fission yeast. EMBO J. **5:**2963–2971.
66. **Fukui Y, Kozasa T, Kaziro Y, Takeda T, Yamamoto M.** 1986. Role of a ras homolog in the life cycle of *Schizosaccharomyces pombe*. Cell **44:**329–336. http://dx.doi.org/10.1016/0092-8674(86)90767-1.
67. **Spyropoulos IC, Liakopoulos TD, Bagos PG, Hamodrakas SJ.** 2004. TMRPres2D: high quality visual representation of transmembrane protein models. Bioinformatics **20:**3258–3260. http://dx.doi.org/10.1093/bioinformatics/bth358.